International Journal of Pharmaceutics 596 (2021) 120198

Contents lists available at ScienceDirect

International Journal of Pharmaceutics

journal homepage: www.elsevier.com/locate/ijpharm

Electrospun tubular vascular grafts to replace damaged peripheral arteries: A preliminary formulation study

Rossella Dorati [a,b,*], Silvia Pisani [c], Enrica Chiesa [a], Ida Genta [a,b], Giovanna Bruni [d], Tiziana Modena [a,b], Bice Conti [a,b]

[a] Department of Drug Sciences, University of Pavia, Via Taramelli 12, 27100 Pavia, Italy
[b] Polymerix s.r.l., Parco Tecnico Scientifico (PTS), Via Taramelli 20, 27100 Pavia, Italy
[c] Immunology and Transplantation Laboratory, Pediatric Hematology Oncology Unit, Department of Maternal and Children's Health, Fondazione IRCCS Policlinico S. Matteo, 27100 Pavia, Italy
[d] Department of Chemistry, Physical Chemistry Section, University of Pavia, Via Taramelli 12, 27100 Pavia, Italy

ARTICLE INFO

Keywords:
Electrospinning
Nanofibers
Tissue regeneration
Polylactide-co-polycaprolactone
Nanofabrication

ABSTRACT

Polymeric tubular vascular grafts represent a likely alternative to autologous vascular grafts for treating peripheral artery occlusive disease. This preliminary research study applied cutting-edge electrospinning technique for manufacturing prototypes with diameter ≤ 6 mm and based on biocompatible and biodegradable polymers such as polylactide-polycaprolactone, polylactide-co-glycolide and polyhydroxyethylmethacrylate combined in different design approaches (layering and blending). Samples were characterized about fiber morphology, diameter, size distribution, porosity, fluid uptake capability, and mechanical properties. Biocompatibility and cell interaction were evaluated by *in vitro* test. Goal of this preliminary study was to discriminate among the prototypes and select which composition and design approach could better suit tissue regeneration purposes. Results showed that electrospinning technique is suitable to obtain grafts with a diameter < 6 mm and thickness between 140 ± 7–175 ± 4 μm. Scanning electron microscopy analysis showed fibers with suitable micrometric diameters and pore size between 5 and 35 μm. polyhydroxyethylmethacrylate provided high hydrophilicity (≃ 100°) and optimal cell short term proliferation (cell viability ≃ 160%) in accordance with maximum fluid uptake ability (300–350%). Moreover, addition of polyhydroxyethylmethacrylate lowered suture retention strength at value < 1 N. Prototypes obtaining combining polylactide-co-glycolide and polylactide-coglycolide/ polyhydroxyethylmethacrylate with polylactide-polycaprolactone in a bilayered structure showed optimal mechanical behavior resembling native bovine vessel.

1. Introduction

Peripheral artery occlusive disease is characterized by high prevalence in general population (4–12% of adults aged 55–70 years-old) with a significant burden of mortality (10–15%), and morbidity. The current treatment options for symptomatic patients unresponsive to optimal medical therapy rely on surgical or endovascular revascularization, depending on extent and location of vascular lesions. In 2015 guidelines, the European Society for Vascular Surgery recommends surgical graft revascularization as first approach to long (>25 cm) or occlusive femora-popliteal lesions in all standard-risk patients. In these cases, autologous vein bypass surgery, most often using great saphenous vein, represents the gold standard option, having a longer durability and higher long-term patency than prosthetic graft. According to recent published literature (Almasri et al., 2018), 3-years-patency rates are 77% vs 56% in femoral-popliteal district and 71% vs 42% in infra-popliteal district. This is mainly due to a better physiological structure of the venous walls, which includes cellular component and organic matrix (e.g., collagen, elastic fibers, etc.), less prone to develop thrombosis than synthetic materials (usually PTFE). However, saphenous veins can be unfit for bypass surgery, mostly because their diameter do not fit properly and they have limited availability. For this reason, new materials mimicking the mechanical and biologic properties of vascular wall tissues, or engineered tissues reproducing vascular histology would represent an optimal solution. This approach provides a virtually unlimited source of physiologic conduits featured by high safety, effectiveness and durability. Unfortunately, as detailed in the following, this need is yet unmet. Tissue engineered vascular grafts (TEVGs) represent

* Corresponding author.

https://doi.org/10.1016/j.ijpharm.2021.120198
Received 23 September 2020; Received in revised form 21 December 2020; Accepted 22 December 2020
Available online 1 February 2021

an alternative to autologous vascular grafts and they are in study to overcome the drawbacks of autologous vascular grafts. The ideal TEVG should be readily available, cost effective, manageable, offering high cell growth capability. Moreover, it should be resistant to development of thrombosis, stenosis, calcification, or infection. The scaling grafts technologies from small to large animal models was very challenging; however, TEVGs clinical translation was greatly anticipated based on their market forces and patient need (Matsuzaki et al., 2019).

TEVGs generally consists of scaffold, cells, and signals which act in synergy to promote tissue repairing or regeneration. Currently, synthetic not biodegradable polymer materials such as Dacron and Goretex (base on PTFE) are used for large and medium diameter vessels (inner diameter (ID) $>$ 6 mm), their application to small diameter vessels (ID $<$ 6 mm) is very difficult presenting a lifetime risk of thrombosis and infection. TEVGs obtained combining biologically active cells with polymer biodegradable scaffolds have potential to overcome these limitations providing optimal cell growth capacity and tissue repairing. Ideally, a vascular scaffold should be composed of a durable biomaterial able to withstand physiological hemodynamic forces maintaining structural integrity until in vivo mature tissue is formed. Materials used for producing of TEVGs are numerous, as decellularized matrices (e.g. porcine abdominal aorta and carotid, human umbilical artery), biodegradable synthetic polymers (e.g. polyglycerol sebacate (PGS), polycaprolactone (PCL), polylactide-co-polycaprolactone (PLA-PCL), polylactide (PLA), PCL blends, polylactide-co.glycolide (PLGA), polyethylenoxide, polydioxanone (PDS) pluronic etc.), natural polymers (fibrin, thrombin and fibrinogen blends, recombinant human tropoelastin, elastin, silk fibroin, chitosan, collagen, gelatin, hyaluronic acid, alginate etc.) (Fitzsimmons et al., 2018; Ong et al., 2017; Pan et al., 2017). Polyurethane can be used as blending with other biomaterials for its superior mechanical properties (Catto et al., 2015). Combinations of natural and synthetic polymers are often studied; natural polymers have higher potential to attract cells into the vascular graft while synthetic biomaterials can better modulate vascular graft mechanical properties (Fukunishi et al., 2016). Cellular component is fundamental in order to achieve cellularized vessel, they can be endothelial cells (EC); smooth muscle cells (SMC), mesenchymal stem cells (Pashneh-Tala et al., 2015). In these years, it was demonstrated the safety of grafts and their ability to recruit host cells and guide their participation in vascular remodeling, opening perspectives to studies on cell free TEGVs (Drews et al., 2020; Yuan et al., 2020).

No cellularized TVGs can be differentiated in self-assembled and scaffold-based; in the second approach, the grafts can be used in human study as natural material- (collagen, gelatin, elastin, fibrin, and silk-fibroin) or synthetic material-based (see above). Natural and synthetic polymers can also be blended to ameliorate features that each category possess on its own.

Different manufacturing techniques can be exploited for producing cell free TVGs, such as electrospinning, freeze-drying and mold casting, solvent casting/salt leaching, phase separation and 3D bioprinting (Cordelle and Mantero, 2020; Yuan et al., 2020). Electrospinning technique has become one of the most frequently used approach; in fact, it is a relatively simple method, it allows the manufacturing of tubular scaffolds, it is featured by high reproducibility and easily scalability. Electrospinning is a technique used to produce nanoscale and microscale polymer fibers through the application of an electric current to a polymer solution. Moreover, fiber orientation can be tuned in order to obtain tubular scaffolds with oriented fibers, improving mechanical stretching properties. This technique is particularly attractive for the production of small diameter fibers with high surface area and porosity, interconnected and oriented pores, three-dimensional network structure mimicking natural blood vessels skeleton structure (Chen et al., 2020; Hu et al., 2020; Joy et al., 2020). There are some fundamental parameters that need to be considered to set up a correct electrospinning procedure i.e. the polymer solution's properties, and the instrument' settings as flow rate, applied electrical potential, working distance, mandrel's rotation speed, spinneret's width and speed, humidity and temperature. Solution and instrument parameters are fundamental to define products final characteristics (mechanical properties, porosity, and pore size distribution, morphology and nanofiber diameter). All these parameters depends on the polymer, or polymers blends (Dorati et al., 2020, 2018; Pisani et al., 2018).

The present research study was planned to design electrospun tubular vascular grafts (TVGs) made from biocompatible and biodegradable polymers such as PLA-PCL, PLGA and polyhydroxyethylmethacrylate (PHEMA) combined in different design approaches (layering and blending) and with diameter $\leq$ 6 mm. While PLA-PCL and PLGA were chosen because of their well-known biocompatibility and biodegradability that make them the most used polymers in drug delivery and tissue engineering, PHEMA was selected because of its hydrophilicity and ability of making hydrogels for cell engineering purposes. PHEMA polymer is biocompatible but not biodegradable, and literature refers of its monomer high toxicity (Spicer, 2020). The TVGs were characterized about nanofiber morphology, size and size distribution, porosity, fluid uptake capability, and mechanical properties. A preliminary biological study was performed for evaluating their biocompatibility and capability of cells to interact with electrospun vascular graft. Going through the detailed characterization, goal of this preliminary study was to discriminate among the TVGs and select which composition and preparation method could better suit tissue regeneration purposes.

To the best of our knowledge, this is the first research project, which evaluated the blending and sequencing layering production approaches combining hydrophobic PLGA, PLA-PCL copolymers and PHEMA as hydrophilic polymer for producing small tubular graft. Nanofiber biodegradable graft in tubular shape and having diameter size $<$ 6 mm were produced exploiting the electrospinning technology. In literature, different papers can be found on the production of polymeric tubular grafts, however, their composition is different from the one here investigated. In the specific, PHEMA has been blended with PLGA copolymer for the following reasons: first, PHEMA polymer is hydrophilic, with abundant hydroxyl group and ester groups in polymer chains, which can accelerate the permeation of physiological fluid into fiber matrix; second, its hydrophilicity improve capability to retain large amount of fluid. PHEMA is widely used as controlled drug delivery system, including protein release, breast augmentation surgery, synthetic skin, and it employed in developing contact lenses. The success of this research would provide a valuable and alternative approach for regenerating small blood vessels in pediatrics or in hand microsurgery.

2. Materials and methods

2.1. Materials

Poly-L-lactide-co-poly-ε-caprolactone (PLA-PCL) 70:30, Resomer LC 703 S, Mw 160,000 Da, glass transition temperature 37 °C and Poly Lactide-co-Glycolide (PLGA) 82:18, Resomer LG 824 S, Mw 33,4283 Da, glass transition temperature 54–60 °C were from EVONIK (Nutrion & Care GmbH, 64,275 Damstad, Germany). Poly(2-hydroxyethyl methacrylate) (PHEMA), Mw 20,000 Da, was from Sigma Aldrich (Milano MI, Italy). Acetone (CH_3COCH_3) analytical grade 99.8%, Chloroform (CHL, $CHCl_3$), Dicloromethane (DCM, CH_2Cl_2) analytical grade 99.9% were from Carlo Erba, (Carlo Erba SpA, Milano, Italy). Acetonitrile (CH_3CN) was from Merck (Merck, Germany). Ammonium phosphate monobasic ($NH_4H_2PO_4$) analytical grade $\geq$ 98%; methanol (MeOH, CH_3OH) analytical grade $\geq$ 99.9%; N,N-dimethylformamide (DMF, C_3H_7NO) analytical grade 99.8%; phosphate buffer saline tablet (PBS); phosphoric acid (H_3PO_4) analytical grade $\geq$ 85%; sodium azide (N_3Na) were from Sigma Aldrich (Milano MI, Italy). Double distilled water was filtered with 0.22 μm, Millipore membrane filters before use (Millipore Corporation, Massachusetts, USA).

3. Methods

3.1. Rheology

Polymer solutions viscoelastic properties were investigated using rotational Rheometer Kinexus Pro+ (Malvern, Alfatest, Milan, Italy) equipped with a temperature control system. Data processing was performed by rSpace software. Analysis was carried out using a flat cone geometry CP4 / 40 (cone angle 1°, diameter 40 mm), equipped with solvent trap for creating thermally stable vapor barrier and limiting any solvent loss during rheological analysis. Polymer solution was placed on the stator plate avoiding stressing samples; the rotor was lowered to a distance of 0.15 mm from the flat cone plate and kept constant for all analysis. Rheological properties of each polymer solution were investigated through three rheological tests: i) oscillatory amplitude sweep test, ii) frequency sweep test, and iii) shear rate ramp test.

The rheological study was performed on polymer solutions in solvent mixture at different solvent and co-solvent ratio and at concentrations of 10, 12.5 and 15% w/v in order to evaluate the spinnability of polymer solution and set up the polymer concentration and solvent system composition. Analysis were carried out at 35 °C (for PLGA and PLGA / PHEMA) and at 22 °C (for PLA-PCL) in order to simulate the temperature values used during electrospinning process.

3.2. Preparation of tubular vascular graft

TVGs were prepared using electrospinning Nanon-01A (MEEC Instruments, Ltd, Ogori-shi, Fukuoka, Japan) equipped with dehumidifier system. Polymers were dissolved in DCM; polymer solution was loaded into a plastic syringe w/o stopper (5 mL Syringe, Luer-Lok™ Tip) and injected through a 22G needle**.** The design of TVGs was assessed considering the concentric layered structure of blood vessel; TVGs prototypes were produced as monolayer and bilayer graft. The monolayer grafts were prepared either using the polymers as such or making a physical mixture of them, while bilayer grafts were obtained by sequential electrospinning of two layers.

The electrospinning operating conditions were as follows: needle-collector distance 150 mm, voltage 30 kV, flow rate 3 mL/h, spinneret speed 50 mm/sec and its width (spinneret lateral movement) 50 mm, (Dorati et al., 2020; Pisani et al., 2018). Spindle, having diameter 6 mm, was chosen on the basis of expected final TVGs diameter, and its rotation speed was fixed at 2500 rpm according previous studies (Dorati et al., 2020). The process was carried out at atmospheric pressure, maintaining temperature and humidity constant (30 ± 3 °C, 20 ± 3%). Samples resulting in continuous and uniform fibers with no beads were selected for further structural, mechanical and biological characterization. Electrospinning time was established at 15 min in order to obtain thin, flexible, and elastic grafts. When bilayers grafts were prepared the total spinning time was maintained constant spinning each layer for 7.5 min. Samples were detached from the spindle; they were stored at 4 ± 1 °C under controlled humidity (33 ± 1%) until further characterization.

The yield of production of each TVGs was calculated and adopted as fundamental criteria to evaluate the quality level of the process. The yield values will be useful to propose an effective and efficient approach to improve the production of TVGs by electrospinning and eventually to scale up the production. Yield data were determined using the following equation:

Yield of production (%) = TVG weight (mg) / theoretical amount of electrospun polymer solution (mg) × 100

Data were expressed as average ± sd, (n = 4).

3.3. TVGs physico-chemical characterization

3.3.1. Morphometric characterization of fibers through scanning electron microscopy (SEM)

Morphometric characterization was carried out by scanning electron microscopy (SEM) combined to Image J software in order to study the microstructural features of electrospun TVG. Samples were submitted to Scanning Electron Microscope (SEM) Zeiss EVO MA10 (Carl Zeiss, Oberkochen Germany). The images were acquired at high voltage (20 kV), in high vacuum, at room temperature and at different magnifications 500X, 3.0 kX and 30 kX. ImageJ was used to investigate fiber diameter, fiber size distribution, pore distribution and fiber orientation analysis.

3.3.2. Wettability and contact angle

TVGs wettability of was determined using DMEM medium. The wettability data can be classified as follow: i) perfect wettability when the contact angle (θ) is equal to zero (0), liquid is parallel to the solid surface, ii) high wettability when $90 < \theta < 0$, iii) low wettability when $90 < \theta < 180$, and iv) no wettability when V is > 180.

Contact angle measurement

Contact angle test was performed by Contact angle meter (Kyowa Interface Science, Made in Japan, model DMe-211Plus). The instrument is equipped with the glass syringe with needle, the base on which the glass slide is placed with sample, the light source and the camera. The system was connected to a computer and the images and values of the contact angle are acquired and processed by the FAMAS software. Once the system was calibrated, the software directly processes the contact angle values using θ/2 method. The tangent method and the curve fitting method can be also used to measure the contact angle. The left, right and apex part of the drop were detected with processing image, the radius (r) and the height (h) of the drop are obtained.

Contact angle was calculated by replacing r and h in the following equations:

$$\mathrm{Tan}\,\theta_1 = \mathrm{h/r} \tag{2}$$

$$\theta = 2\arctan \mathrm{h/r} \tag{3}$$

The distance between the syringe and the base is set at 1 cm; in order to have comparable evaluations, the volume of the drop was set to ~1–2 μL. Software acquired the values and the images of the contact angle in triplicate, after 1, 5 and 9 s by the time that the drop was exposed to TVG surface. The contact angle was calculated on both internal and external matrix surfaces. Samples were appropriately cut into squares of ~0.8 × 1 cm, (n = 3).

3.3.3. Mechanical properties

Mechanical properties included *burst pressure strength test*, *tensile properties* evaluation in dry and wet experimental conditions and *suture test*.

The *burst pressure strength* was measured by increasing the pressure through the tubular vascular graft in steps of 375 mmHg for 10 s at each step until 1500 mmHg was reached. The test was performed triplicate and data were compared with those reported in the literature (Wise et al., 2011) for native vessels and previous studies. Sample diameter variation was measured by millesimal digital caliper during the pressure strength test.

Tensile measurements were carried out using dynamic mechanical analysis machine (MARK-10) equipped with 20 N load cell. All analysis were performed on TEVG samples cut into rectangles (2 × 3 cm). Each sample was fixed by two clamps in a way to expose 2 × 1 cm surface, upper clamp moves upwards at controlled speed of 30 mm / sec until sample broke out. All analyses were performed with a pre-load of 0.05 N. Collected data were processed and mechanical properties were expresses as young's Modulus, yield strength, breaking point, ultimate tensile strength (UTS) and percentage elongation.

Suture retention strength was evaluate using dynamic mechanical analysis machine (MARK-10) equipped with 20 N load cell. TVGs were cut in rectangular shape (3 × 1 cm). One end of TVG sample was clamped at onto the dynamic mechanical analysis machine; following, the TVG sample was sutured with two surgical stitches to bovine native blood vessel cut into a rectangle shape (2 × 1 cm) using silk suture thread (2–0 seta mersilk, Pema-hand seide, Ethicon®). Each stitch was placed 2 mm from the edge of the specimen using a curve needle. A constant pulling rate of 30 mm/sec was applied until the suture was pulled out; all analyzes were performed with a pre-load of 0.05 N. The maximum force of pulling that kept suture integrity was recorded as the suture retention strength, (n = 4).

3.3.4. Fluid uptake capability

The TVG fluid uptake capability was measured gravimetrically using an analytical balance (Entris, Sartorius, Gottingen, Germany), the test was performed on cylindrical graft of about 0.8 mm, in quadruplicate. All samples were incubated in DMEM (1.5 mL) and following they were stored at 37° C, in static condition. The culture medium was collected at scheduled time (4, 6, 24, 72 and 120 h), each sample was recovered and TVG diameter was measured using a digital caliper. Fluid uptake capability was expressed as the TVG percentage of weight variation during incubation in DMEM, at 37 °C, (n = 4).

3.3.5. Culture medium pH determination

TVG samples were soaked in complete DMEM (1.5 mL, pH 7.98) in order to evaluate pH shifts during incubation. At scheduled time (4, 6, 24, 72 and 120 h), the culture medium was collected and pH measured by 827 pH lab pHmeter (Methron ion analysis, Switzerland); results are expressed as average ± standard deviation, (n = 4).

3.3.6. In vitro degradation study

An *in vitro* test was set up in order to assess tubular graft degradation behavior in simulated physiological conditions of TVG.5 sample. each patch sample was incubated for 60 days in PBS (7 mL9, pH 7.4, at 37 °C, supplemented with NaN_3 (0.01% w/v) in order to prevent microbiological contamination. The incubation medium was discarded and replaced by fresh medium every other day. At 7, 14, 21, 30, 45, and 60 days of incubation, specimens were collected, freeze-dried (Freeze dryer Lio-5P, Cinquepascal, Italy, at − 48 °C and 0.4 mbar for 12 h) and analyzed by Gel Permeation Chromatography. Data (Mw, Mn and PDI) were expressed as average ± standard deviation (n = 5).

GPC analysis

GPC solutions were prepared dissolving each sample in THF solvent HPLC grade, before injection teach solution was filtered through a0.45 mm filter (Millipore, MA, USA). GPC eluent was tetrahydrofuran at a flow rate of 1 mL/min. GPC apparatus consisted of a guard column (Phenogel 10E 4 Å μm, 300 × 7.8 mm, Phenomenex, Milan, Italy) and two Phenogel 10E 3 Å μm and 500 Å columns connected in series, a pump (Varian 9010, Milan, Italy), a Prostar 355 RI detector (Varian Milan, Italy), and software for Mw distribution computing (Galaxie Ws, ver. 1.8 Single-Instrument, Varian Milan, Italy).

3.4. In vitro biological study

3.4.1. Fibroblasts culture and growth

Human fibroblasts culture derives from human dermis were stored in liquid nitrogen in sterile cryogenic vials. Cell were suspended in DMEM containing 20% v / v of fetal bovine serum (FBS) and 1% v / v of antibiotics (100 μg/ mL penicillin, 100 μg/mL streptomycin) and DMSO (10% v / v). The cell suspension was defrosted and following centrifuged at 1500 rpm for 5 min. The cell pellet was suspended in fresh medium (DMEM containing 20% of FBS and 1% of antibiotics) and incubated at 37 °C and 5% of CO_2 with a relative humidity of 95%.

3.4.2. Samples preparation and cell seeding

In vitro biological study was performed on all TVGs cut into small cylinder at diameter 1 cm and placed in sterile 12-multiwell, all samples were sanitized by exposing overnight to UV lamps under laminar flow hood, at room temperature. All samples were transferred to sterile wells and washed with 60% ethanol for five minutes and subsequently they were conditioned in DMEM 10% v/v (4 mL) for other five minutes. Cell suspension containing 3.5×10^4 cells was seeded on the surface of each TVG (100 μL), samples were maintained under laminar hood for almost 20 min in static conditions with no addition of fresh medium in order to facilitate the attachment of cells. Fresh medium (3.5 mL) was added to each well and samples incubated at 37 °C, 5% CO_2. The attachment was evaluated after incubation for 6 h, while proliferation study was assessed after 3 and 5 days. Cell viability was evaluated on three samples for each eGV and eGV with no cells and cells cultured in 2D (bottom of well) were used as negative (CRT−) and positive (CRT+) control, respectively.

3.4.3. MTT assay

The assay with 3- (4, 5-dimethylthiazol-2-yl)-2,5-diphenyltetrazolium bromide (MTT) was performed to evaluate cells culture viability and proliferation capacity of cells seeded on TVGs. At prescheduled times, the culture medium was eliminated and replaced with DMEM without serum; subsequently, 100 μL of MTT solution (5 mg/mL in sterile DMEM w/o FBS) were added to each well plate. All samples were incubated for 2.5 h at 37 °C to allow the reaction of MTT reduction by mitochondrial dehydrogenase of viable cells and later the medium was removed, and the samples were carefully washed with PBS, in order to eliminate residues of medium and unreacted MTT that could interfere with the reading spectrophotometric. TVGs samples were dissolved in tetrahydrofuran (THF, 1 mL) under magnetic stirring speed in ice-water bath; THF has been identified as the most suitable solvent for the solubilization of TVG nm wavelength in a quartz cell (6705 UV/Vis Spectrophotometer – Single cell holder JENWAY), THF was used as blank. Solutions were analyzed at 570 nm (microplate Reader Model 680, bio-Rad Laboratories, USA) with 655 nm as wavelength. Results of cellular viability were expressed as UV–Vis absorbance of TVG samples compared with the positive control absorbance (CRT+). The negative control (CRT) was necessary to exclude the polymer interference in the UV–vis reading.

4. Results and discussion

4.1. Electrospinning TVGs design through rheological analysis

Results of rheological analysis combined to Berry's number evaluation and viscosity's surface tension determination, led to choose PLGA solution 15% w/v as long and PLA-PCL 15% w/v and PLGA 15%/PHEMA 5% as the most useful concentrations in the binary solvent: cosolvent systems CHL:DMF 80:20 and DCM:DMF 80:20, since the high viscosity values and viscous behavior should facilitate jet initiation and elongation. Moreover, at these concentrations the jet ensured continuous movement away from the nozzle with reduction of cleaning cycles that led to higher process yield.

Fig. 1**a** reports and compares results of rheological analyses performed on selected PLGA and PLA-PCL solutions at concentration 15% w/v, and PLGA/PHEMA 15%/5% w/v in the binary solvent system CHL: DMF 80:20. Shear viscosity was measured as a function of shear rate for each polymer solution over a wide range of shear rates (1–100 s^{-1}) using a rotational rheometer. The viscosity values, at low shear rate, were consistent with polymer Mws. The highest viscosity values were obtained for PLGA 15% w/v solution and PLGA/PHEMA, 15%/5% w/v blend, while PLA-PCL 15% w/v solution showed lower viscosity. All the polymer solutions exceeded critical overlap concentration identified in preliminary rheological study performed on diluted polymer solutions (see supplementary data). Cohesive energy values, calculated by G' and

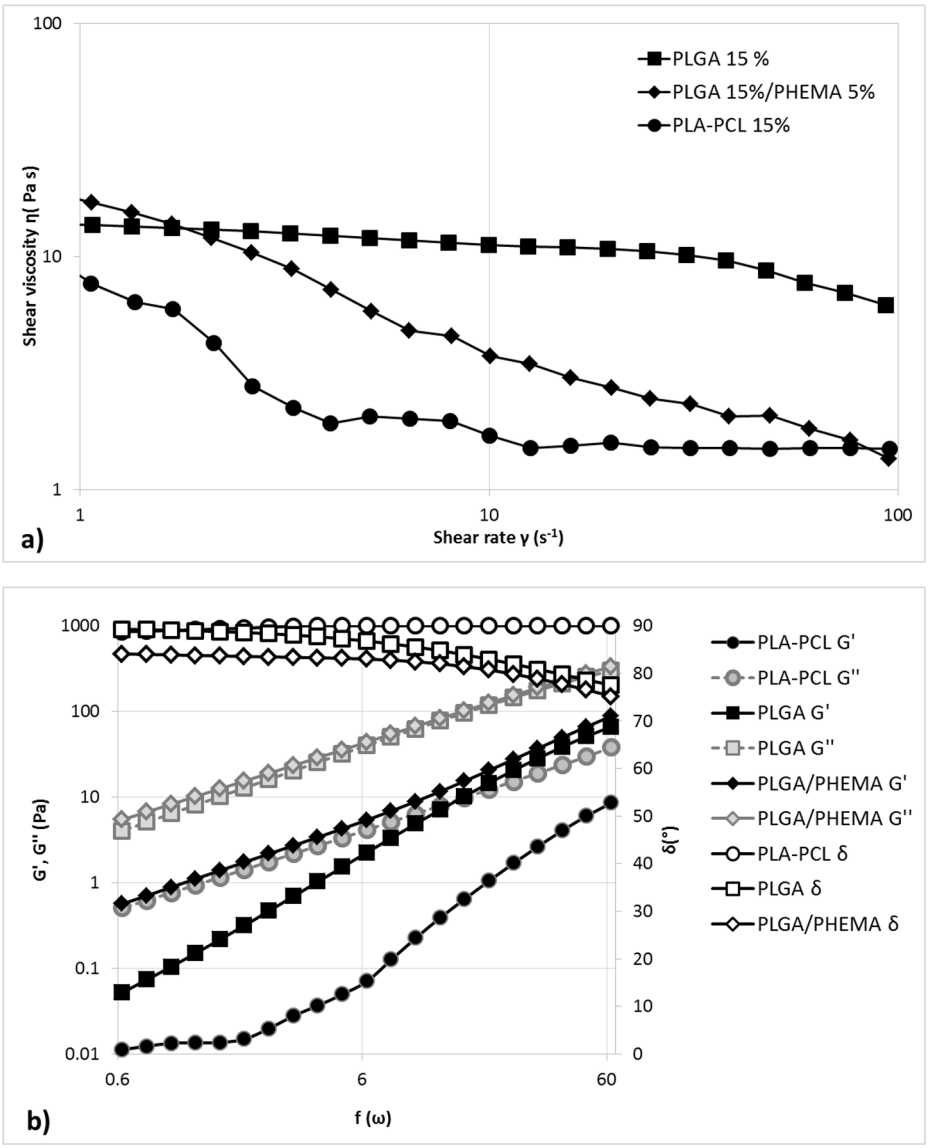

Fig. 1. a) Viscosity profiles for the selected polymer solutions: PLGA 15% w/v (*dark solid square*), PLGA 15%/PHEMA 5% %w/v (*dark solid diamond*), PLA-PCL. 15% w/v (*dark solid circle*); and their **b)** Dependence of storage modulus G' (*dark solid marker, solid line*), loss modulus G'' (*grey solid marker, dashed line*) and loss tangent tan δ (*dark open marker, solid line*) on frequency.

γ at max LVER region, indicates that the PLA-PCL solution had the highest elastic strength of the internal structure and is in correlation with the yield stress, which is the value of the shear stress at the limit of the LVER region. The frequency sweep test highlighted the predominantly viscous nature of all polymer solutions; all solutions have liquid viscoelastic behavior since G'' > G' and tang δ is ~79–90° (Fig. 1**b**).

4.2. TVGs preparation and morphometric characterization

On the basis of results of rheological analysis the most suitable binary solvent systems were CHL:DMF and DCM:DMF, with ratio value 80:20 for all polymers and blends. Table 1 summarizes the composition of TVGs obtained with selected polymer solutions. TVGs sizes were 5.85 ± 0.43 mm internal diameter (Fig. 2) while wall thickness ranged between 140 ± 7.0 μm and 175 ± 4.0 μm as measured by caliper and reported in Table 2. The variability of wall thickness of TVGs samples could be partly associated with yield process and fiber structure.

In 2018, Yalcin et al. reviewed design parameters for electrospun vascular grafts and reported heterogeneity in artery and blood vessels wall thickness as long as wall to lumen (W:L) ratio which resulted to be higher in small vessels. This parameter well correlates to burst pressure values, which increased as wall thickness increases (Yalcin Enis and Gok Sadikoglu, 2016).

Table 1
TVGs type, composition and polymer concentration.

Batch #	Layer composition		Binary solvent system composition	
	Polymer type (%, w/v)			
Monolayer	**1st***	**2nd**	**1st***	**2nd**
TVG.1	PLGA (15)	–	CHL:DMF	–
TVG.2	PLGA/PHEMA (15/5)	–	DCM:DMF	–
TVG.3	PLA-PCL (15)	–	CHL:DMF	–
Bilayer	**1st***	**2nd****	**1st***	**2nd****
TVG.4	PLGA (15)	PLA-PCL (15)	CHL:DMF	DCM:DMF
TVG.5	PLGA/PHEMA (15/5)	PLA-PCL (15)	CHL:DMF	DCM:DMF

The yield process was calculated for each prototype and expressed as average ± sd of five samples; the results demonstrated fairly low yield production percentages, ranging from 40.60 to 62.96%. The lowest process yield value was measured for tubular vascular grafts containing

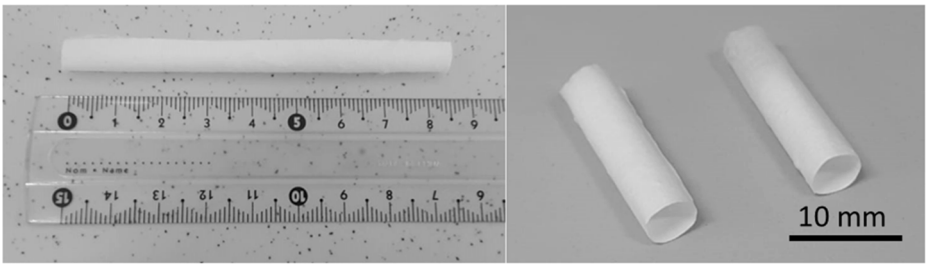

Fig. 2. Macrographs of TVG.4 length and internal diameter (ID) of 5.85 ± 0.43 mm tube.

Table 2
TVGs morphometric characterization with regard to mean diameter, fiber diameter range, porosity, and yield of production.

Batch #	Mean diameter (μm)	Fiber diameter range (μm)	Porosity (%)	Thickness (μm)	Yield of production (%)
Monolayer					
TVG.1	5.0 ± 1.8	2–26	49.85 ± 5.5	140 ± 7.3	62.96
TVG.2	5.5 ± 3.6	2–42	50.19 ± 7.2	155 ± 6.5	60.88
TVG.3	3.2 ± 0.7	2–28	46.0 ± 5.7	176 ± 4.0	40.60
Bilayer					
TVG.4	1.12 ± 0.2*	1 – 36	51.6 ± 6.6	175 ± 4.2	56.18
TVG.5	4.1 ± 0.3*	2–32	50.5 ± 4.5	143 ± 2.9	35.91

PHEMA (TVG.2 and TVG.5). Explanation of this is that Taylor cone and jet were extremely unstable over time for PLGA/PHEMA blends and in these conditions numerous cleaning cycles are required for removing polymer clumps formed at nozzle top. Fig. 3 shows some representative SEM images of monolayer TVGs (TVG.1, TVG.2 and TVG.3). SEM images show smooth, bead less, and interconnected fibrous graft with random fiber distribution and fiber diameters in the microscale range (Table 2).

SEM analysis of bilayer tubular graft (TVG.4 and TVG.5, Fig. 4) confirmed the structure of a dense external layer with porosity ~ 50%. The specific feature highlighted by scanning electron microscopy is partial fusion on fiber at the edge between the two layers (Fig. 4**d**); this evidence has been attributed to partial softening of PLGA polymer chains on the surface of fibers (1st layer, internal side) when PLA-PCL wet fibers (2nd layer, external side) are collected. Specifically, the average fiber diameter was around 8.0 ± 1.8 μm for TVG.1, TVG.2, TVG.3 and TVG.5: and it ranged from 2.0 to 42 μm. The narrower diameter distribution was observed for TVG.1 and TVG.3 monolayer tube. Fiber orientation was verified by ImageJ software using OrientationJ Plugin; fibers are steadily spread between −90 and 90° confirming the random morphology of the fabricated membrane (data non reported).

The porosity percentage determined by ImageJ software indicated that tubular TVGs had a porosity ranging from 46 ± 5.7 and 51.6 ± 6.6%. The pore size was distributed between 5 and 35 μm, with a mean value of ~12.18 ± 3.13 μm. Pore size is a fundamental parameter for vascular grafts. The ability of fiber vascular grafts to support cell adhesion and proliferation depends on porosity percentage, pore size and their size distribution. Mimicking ECM is one of the advantages of electrospun vascular grafts owing to the topography created by fibers and interconnected pores resulting in a large surface area that promotes endothelium formation and prohibits arterial thrombosis. It is well known that attachment and proliferation of endothelial cells (EC) is improved on fibers with diameters smaller than the cell diameter (<5 μm). On the other hand, the controllable pore size and porosity of electrospun scaffolds allow smooth muscle cells (SMCs) to grow, migrate, and regenerate through the scaffold via creating large spaces

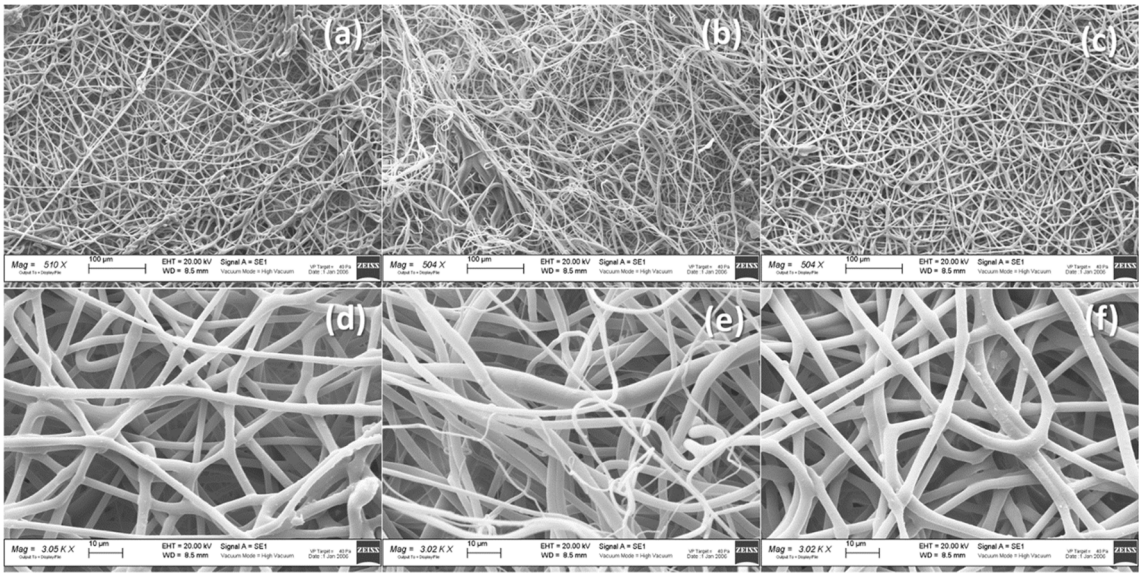

Fig. 3. SEM images of monolayer TVGs samples: TVG.1 (a, d), TVG.2 (b, e) and TVG.3 (c, f), magnification 510X and 3.0 kX.

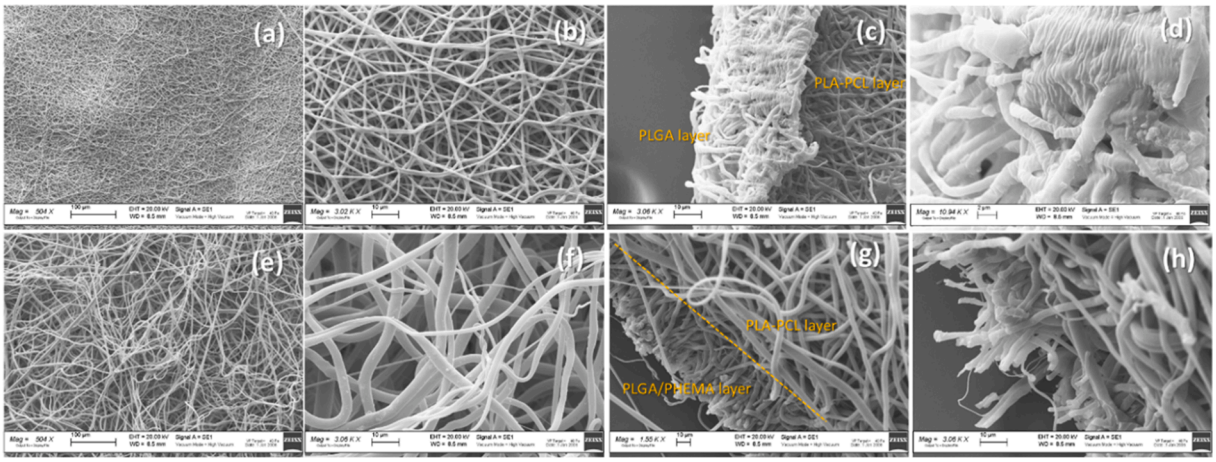

Fig. 4. SEM images of TVG samples: TVG.4 (a-d) and TVG.5 (e-h), magnification 510X and 3.0 kX.

(>5 μm to allow cell diffusion). The pores must allow infiltration of SMCs while hindering blood leakage. Multilayer or single-layer vascular grafts can be considered interesting technique also to achieve bimodal porosity. Nanofibrous layer with nano pore sizes served as an improved surface for EC attachment; moreover, fiber diameter of ~1 μm was determined as the sub limit in the outer layer for SMCs infiltration. Similarly, it was stated that the inner layer with lower porosity reduced blood leakage promoting cell penetration from the outer layer (through higher porosity). Nevertheless, cell invasion and neovascularization were significantly reduced in grafts composed of lower porosity structure in the outer layer, as reported in the literature (Fioretta et al., 2012).

4.3. Wettability and contact angle

Fig. 5 depicts values of contact angle determined on the internal and external surface of TVGs; test was performed using DMEM as fluid. The internal contact angle of TVG.2 (67.43 ± 8.66°) was significantly lower than that of external TVG.2 (95.20 ± 2.23°) and TVG.3 (95.02 ± 1.05°), indicating that the TVG.2, based on physical mixture of PLGA and PHEMA had more hydrophilic nature compared with TVGs compositions based on PLGA and PLA-PCL. This is mainly due to the presence of hydrophilic PHEMA polymer chains, which are able to form hydrogen bond with water, thus showing higher wettability than pure PLGA and PLA-PCL TVGs. Contact angle values ~100° were observed for bilayer TVG.4 and TVG.5. Results were expected for TVG.4 made from the hydrophobic polymers PLGA and PLA-PCL, while the contact angle value of TVG.5 internal surface is significantly lower than that of external layer because internal layer contains PHEMA (see compositions reported in Table 2). Different values obtained for internal surfaces of monolayer and bilayer TVGs can be attributed to interaction of the different polymers making the two layers, as highlighted by SEM partial fusion on fiber at the edge between the two layers, and the prevalence of hydrophobic polymers in TVG.5 composition with respect to TVG.2.

4.4. Mechanical properties

Mechanical properties included the results of pressure strength test,

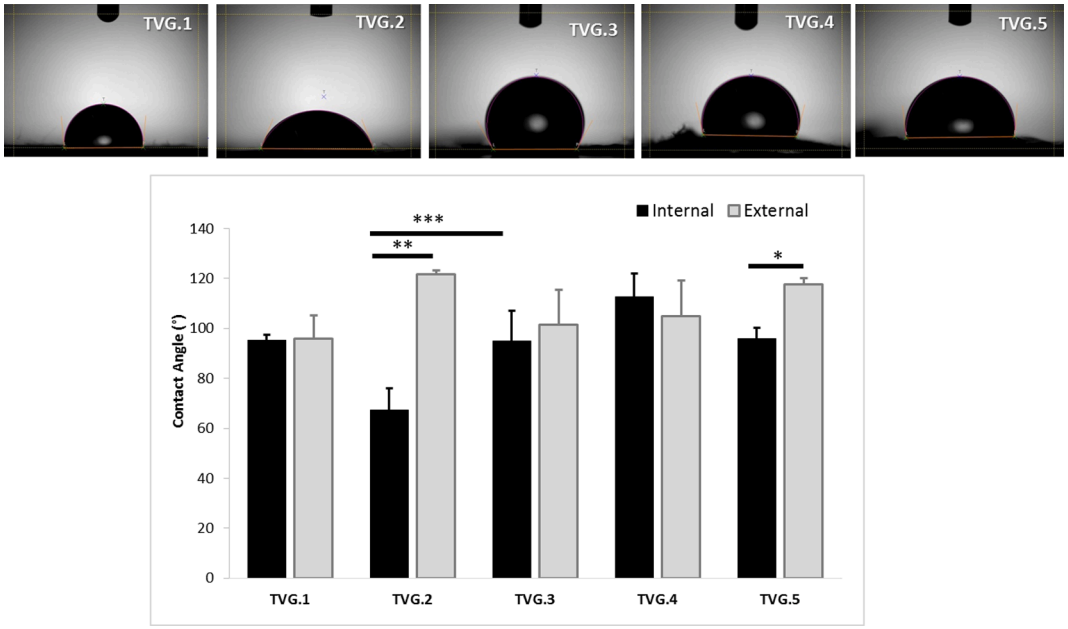

Fig. 5. Contact angle values of TVGs samples. Contact angles were determined on internal and external surface of tube; on the top, representative images of internal surface measurements. Each measurement was made in triplicate, and data represented the means ± SD. A probability value less than 0.05 (*p < 0.05) was defined to be significant and 0.01 (**p < 0.01), 0.001 (***p < 0.001), 0.0001 (****p < 0.0001) as highly significant by Tukey's multiple comparison test.

tensile properties evaluated in dry and wet experimental conditions and suture test. Pressure strength test evaluated variation of TVGs diameter vs applied increasing pressure; the data are plotted as diameter values (mm) over pressure (mmHg) in Fig. 6**a**. The values at zero mmHg pressure correspond to the internal diameter of TVGs, ranging between 5.57 and 5.72 mm; the diameter of all TVGs slightly increased up to 5.87 mm when pressure was applied. The diameter of TVGs based on PLA-PCL linearly increased with pressure; the highest variation of diameter (2.8%) under pressure was measured for monolayer TVG.2 containing PHEMA polymer. The diameter of TVGs looked jagged when sample was tested at maximum pressure value, i.e. 1500 mmHg; furthermore, deformation was irreversible over the time.

Burst pressure is clearly one of the key parameters that determines a vessel's suitability for implantation. All TVGs bore increasing pressure up to 1500 mmHg without rupture. Considering burst pressure results, no dependency neither on polymer composition nor on the TVGs structure (mono- and bi-layer) was found; all TVG samples are capable to hold up against ~2 bar (1500 mmHg). Furthermore, the TVGs developed in this research study bore up to a pressure value higher than upper pathological pressure (180–220 mmHg), and equal to native human saphenous veins (~1500 mmHg) (Wise et al., 2011). Several research groups have recently reported burst pressures for tissue engineered blood vessels exceeding 2000 mmHg; these results should take in consideration both the geometry of the analyzed specimen, their diameter and longevity (Chue et al., 2004; Konig et al., 2009; L'Heureux et al., 2006; Nieponice et al., 2008).

Representative stress/strain curves obtained by tensile mechanical tests exhibit different behavior, depending on structural features and composition of TVG samples (Fig. 6**b**). Two different regions could be detected in the stress / strain curves; in the first zone, the highest Young's modulus (highest curve slope) is recorder for TVG.1 and eTVG.2 based on PLGA and PLA-PCL copolymer, respectively. The tensile properties of TVGs are reported in details in Table 3, showing the most promising results for TVG.4 characterized by an elastic modulus of 0.01 ± 0.01 MPa, yield strength of 0.14 ± 0.20 MPa, UTS 0.17 ± 0.22, breaking point 0.15 ± 0.20 MPa and elongation % of 251.1 ± 188.6. All these values are close to mechanical properties of native vessel. No statistical differences were observe between results of specimens in dry and wet conditions (Table 3). Suture retention strength of TVGs (TVG.1 – TVG.5) ranged from 0.58 ± 0.35 N and 2.84 ± 0.72 N.

Table 3
Tensile properties of TVGs in dry and wet experimental conditions: young's modulus, yield strength, UTS, breaking point and elongation percentage.

Dry conditions					
Batch #	**Young's Modulus (MPa)**	**Yield strength (MPa)**	**UTS (MPa)**	**Breaking point (MPa)**	**Elongation (%)**
Monolayer					
TVG.1	0.3 ± 0.1	0.96 ± 0.52	1.01 ± 0.6	0.91 ± 0.54	135.9 ± 3.3
TVG.2	0.56 ± 0.10	0.79 ± 0.9	0.76 ± 0.86	0.69 ± 0.78	99.4 ± 14.9
TVG.3	0.97 ± 0.02	0.05 ± 0.02	0.08 ± 0.04	0.05 ± 0.06	211.5 ± 2.2
Bilayer					
TVG.4	0.02 ± 0.003	0.13 ± 0.10	0.15 ± 0.09	0.14 ± 0.09	571.7 ± 1.1
TVG.5	0.32 ± 0.09	3.17 ± 0.96	3.08 ± 0.97	2.77 ± 0.87	346.7 ± 7.1
Wet conditions					
Batch #	**Young's Modulus (MPa)**	**Yield strength (MPa)**	**UTS (MPa)**	**Breaking point (MPa)**	**Elongation (%)**
Monolayer					
TVG.1	0.28 ± 0.1	1.44 ± 1.27	1.40 ± 1.0	1.26 ± 0.9	199.4 ± 7.2
TVG.2	0.25 ± 0.33	0.11 ± 0.01	0.13 ± 0.01	0.11 ± 0.01	93.9 ± 22.8
TVG.3	0.01 ± 0.01	0.063 ± 0.04	0.97 ± 0.07	0.09 ± 0.06	292.8 ± 3.4
Bilayer					
TVG.4	0.01 ± 0.01	0.14 ± 0.2	0.17 ± 0.22	0.15 ± 0.2	251.1 ± 8.6
TVG.5	0.20 ± 0.14	1.10 ± 0.66	2.12 ± 0.16	1.91 ± 0.15	524.7 ± 9.3
Control Native bovine vessel	**0.04 ± 0.005**	**0.18 ± 0.09**	**0.46 ± 0.4**	**0.17 ± 0.09**	**222.6 ± 0.5**

In Fig. 6**c** are collected few representative images captured during the suture retention strength test. Retention strength values were significantly different ($p < 0.05$) among TVG.1, TVG.2 and TVG3, while no significant differences were highlighted between TVG.2 and TVG.5,

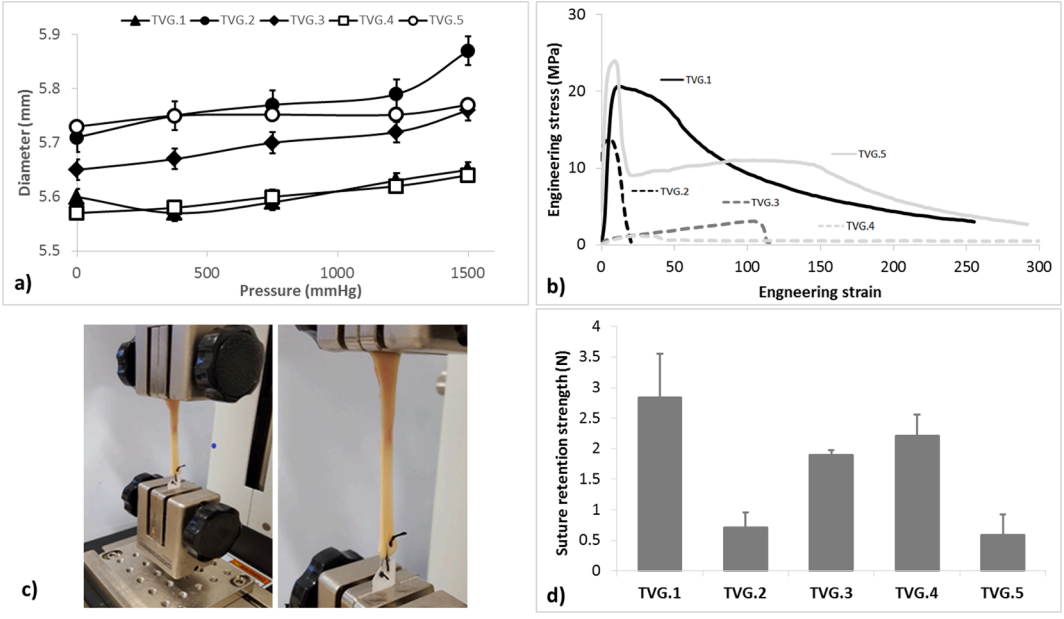

Fig. 6. Results of mechanical tests: **a)** Diameter changing vs pressure; **b)** representative tensile tress-strain curves of TVGs; **c)** representative images of prototype during suture test and **d)** suture retention strength values for each TVG.

and TVG.3 and TVG.4. These findings could be ascribed to TVGs polymer composition and are consistent with their mechanical features; addition of PHEMA resulted in lowering suture retention strength at value < 1 N, while mono and bilayer TVGs based on PLGA exhibit highest suture retention strength ranged from 2.20 ± 0.35 and 2.84 ± 0.72 N. No statistically significant differences were highlighted between monolayer TVG.1 based on PLGA, and bilayer TVG.4 obtained combining PLGA layer and PLA-PCL one (Fig. 6**d**).

4.5. Fluid uptake capability

Fluid uptake capability was determined for all TVGs and it was expressed as percentage of weight variation during incubation in DMEM, at 37 °C. The fluid uptake equilibrium was obtained after incubation for 6 h, no further important increases were observed during all incubation time. The highest fluid uptake percentages ranged from 300 to 350% were observed for bilayer TVGs (TVG.4 and TVG.5) and monolayer TVG based on PLGA (TVG.1), while monolayer TVGs obtained blending PLGA with PHEMA or PLA-PCL exhibited limited fluid uptake capability compared to TVG.1, TVG.4 and TVG.5.

At the same time, physical stability of all TVGs was evaluated measuring their diameter variations during the incubation in cell culture media, DMEM at 37 °C. Consistently with the results of fluid uptake capability, the highest diameter variation percentage (8.0–13%) was determined for TVG.4 and TVG.5 characterized by bilayer structure, porosity percentage > 50% and fiber diameter between 2 and 4 μm (see Table 2). Diameter variation percentages < 6% were measured for monolayer TVGs (TVG.1, TVG.2 and TVG.3); limited changes in diameter (<2%) were assessed for monolayer TVGs obtained blending PLGA with PHEMA (TVG.2) or PLA-PCL (TVG.3).

4.6. In vitro degradation study

Degradation profile of TVG.5 prototype incubated in PBS at pH 7.4 is reported in Fig. 7a, data showed a gradual degradation of polymer matrix at day 7 of about 15% and reaching 42% reduction in 56 days. Polydispersity index values increased in correspondence to Mw decreasing, data are in line with the breaking of PLA-PCL and PLGA chains in low-Mw oligomers (see Fig. 8).

Fig. 7b shows the logarithmic plot of Mwt/Mw0 versus time for TGV.5 sample, degradation rate constant (k) and half-life times ($t_{1/2}$) were calculated using following equations:

$$\mathrm{Ln}\,\mathrm{Mwt/Mw0} = -\mathrm{kt}$$

$$t_{1/2} = 0.6931/k$$

where Mwt is the weight-averaged molecular weight at time t, Mw0 is the weight-averaged molecular weight at time zero, k is the apparent degradation rate and $t_{1/2}$ is the half-life time of degradation. Kinetics results show that TGV.5 degradation rate constant was 1.27×10^{-2} day^{-1} half-life time of about 77 days.

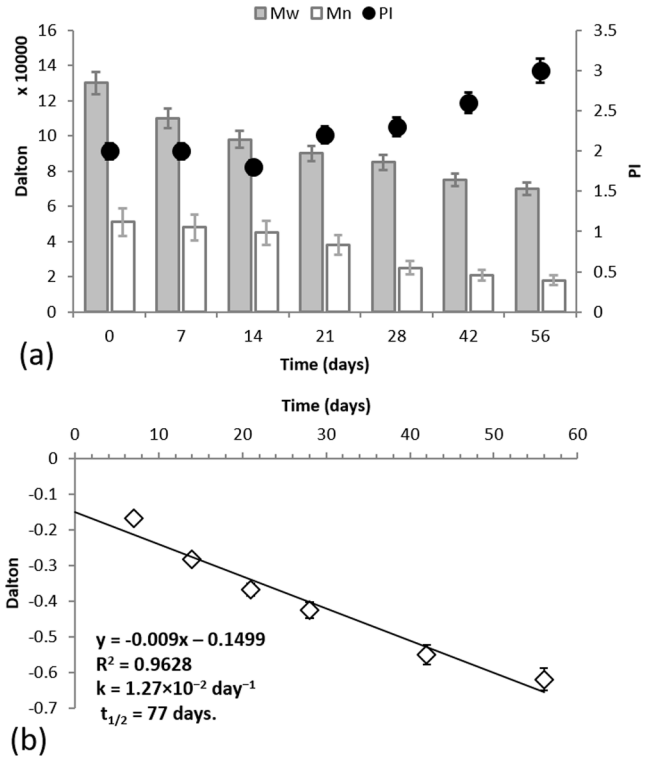

Fig. 7. First-order plots of the degradation ofTVG.5 in PBS at pH 7.4, 37 °C. First order equation, regression coefficient, degradation rate (k, day^{-1}) and half-life ($t_{1/2}$, day) obtained from first-order plot.

4.7. Culture medium pH determination

When TVGs were incubated in a culture medium i.e. for *in vitro* engineering process, its pH value could influence biological and biochemical reactions, namely cell wellness and growth. PH shifts during incubation in a culture medium could be caused by degradation of TVGs themselves, since they are made from biodegradable polymers. In this case, a shift toward acidic pHs is expected. DMEM pH is assessed to be 7.4 in 10% CO_2, these conditions take place in a cell incubator. In absence of CO_2 starting DMEM pH is basic because of the presence of sodium bicarbonate. Results of pH determination in the culture medium showed values ranging from ~ 8.0 to 9.3; the maximum pH value was reached after almost two days of incubation in DMEM at 37 °C, in static conditions; while at the 3rd day, pH values were slightly reduced up to

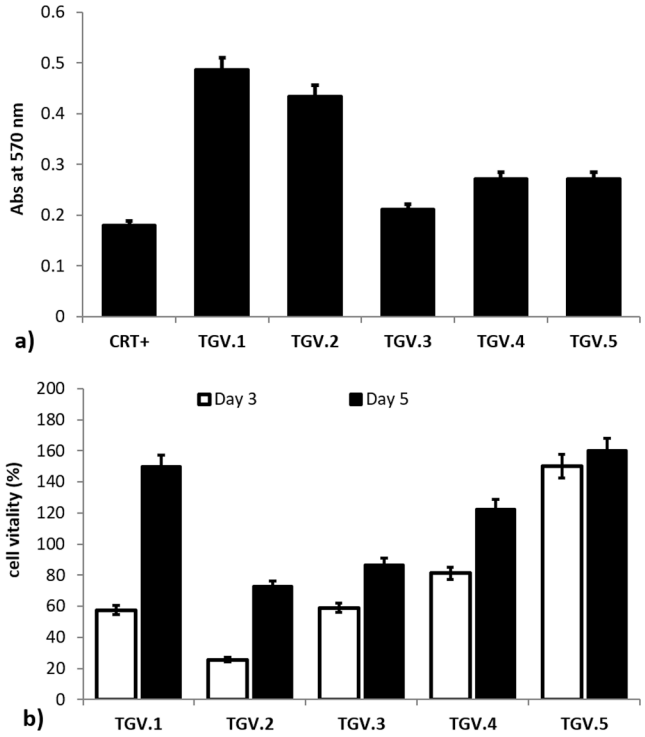

Fig. 8. MTT Assay; **a)** attachment of cell seeded on surface of TVG prototypes and **b)** cell growth of cells on samples during incubation at 37 °C and 5% CO_2. All data are expressed as average ± sd, (n = 3). The proliferation data are expressed as cell vitality percentage compared to control and normalized vs growth area (4 cm^2), which correspond to the area for growth of 12-well multiwell.

8.7–8.9. No significant variations were highlighted among the different TVGs tested. These results confirmed no impressive degradation of polymers making TVGs in 120 h.

4.8. In vitro biological study

Preliminary results of cell attachment and short-term proliferation were obtained by MTT assay after 6 h and 5 days of incubation respectively.

MTT results demonstrated higher attachment of cells on TVGs with respect to CRT+, which can be interpreted as better cell attachment on 3D structures (TVGs) with respect to the 2D ones (CRT+). In details, MTT assay demonstrated higher attachment of cells on TVG.1 and TVG.2 samples compared with TVG.3-TVG.5, Fig. 7**a**. The results of short-term cell proliferation, plotted in Fig. 7**b,** are expressed as Abs percentage (%) vs CRT+ and were determined as cells growth at day 3rd and 5th on the surface of TVG samples. Gradual and consistent cell growth over time was highlighted on TVGs, at day five the best cell proliferation was detected on monolayer TVG sample (TVG.1) based on PLGA polymer, and bilayer TVG samples (TVG.4 and TVG.5). The results can led do affirm that: TVGs are suitable structure for cell adhesion and proliferation, but their composition plays an important role for cells. In particular, PLGA and its ternary blend/layering with PHEMA and PLA-PCL resulted to be the best polymer composition favoring cell proliferation.

5. Discussion

The topic investigated in this project is extensively debated in the literature. The goal of all these studies was to produce small diameter acellular tubular vascular grafts which satisfy as much as possible the main requirements of well-matched mechanical properties, blood compatibility, endothelialization and biodegradability: the four properties ultimately contribute to achieve tubular vascular grafts patency (Li et al., 2019; Wang et al., 2017; Wu et al., 2018)

In the present study, results of physical–chemical and preliminary biological characterization permit to discuss and compare the properties of the TVGs obtained, in order to select which composition and preparation method could better suit tissue regeneration purposes.

Addition of PHEMA to the TVGs formulation provided higher hydrophilicity as shown by higher contact angle values. In particular, the presence of a layer made from PHEMA resulted in the highest values of cell short term proliferation. This result is consistent with the higher fluid uptake ability. However, addition of PHEMA lowered suture retention strength, while mono and bilayer TVGs based on PLGA exhibited the highest suture retention strengths. Consistently monolayer TVGs based on PLGA and bilayer TVGs made from PLGA and PLA-PCL resulted in the best mechanical properties in terms of Young modulus, more resembling that of native bovine vessel, but with lower UTS value. On the contrary TVGs composition made of PLGA and its ternary blend/layering with PHEMA and PLA-PCL (TVG5) resulted in the highest UTS value.

Addition of PHEMA resulted to significantly affect TVGs mechanical properties. Since no paper has been found in the literature on similar TVGs composition including PHEMA, these results have been compared with those obtained by Zhang and coll. and by K.A. McKenna and coll. (McKenna et al., 2012; Zhang et al., 2019). Both authors investigated small-caliber vascular grafts from collagen filaments and from tropoelastin respectively, and their results are in keeping with those found in the present work, demonstrating that addition of hydrophilic polymers such as PHEMA is promising but needs to be further investigated.

On the other hand, PLGA, and PCL are consolidated biomaterials used in tissue engineering approach and experimented for small vascular graft fabrication, as demonstrated by the huge literature (Lee et al., 2008; Li et al., 2019; Wang et al., 2020). Wang and coll. in a systematic experimental study, evaluated the mechanical properties of multiple layer electrospun PLGA small diameter vascular grafts, demonstrating that burst pressure and suture retention increase, elastic tensile modulus maintains unchanged statistically, with the increase of layer number (Wang et al., 2017). The values Young modulus obtained by Wang and coll. are in keeping with the results obtained in the present work for TVG1, while suture retention strength value found in the present work is at least 10 times higher than those found by Wang and coll. The difference in the suture strength values is because this value depends on the number of electrospun PLGA layers, while Young modulus depends mainly on the type of polymer.

PCL is an interesting biomaterial, due to its high biocompatibility and low biodegradation rate, but it is usually combined with other polymers such as PLA, in order to get suitable mechanical properties, as a balance between the stiffer PLA and softer PCL, and to modulate its degradation rate (Buscemi et al., 2017; Li et al., 2017; Vaz et al., 2005). As an alternative, the use of the copolymer PLA-PCL has been scarcely reported in the literature. In example, He and coll. tested the mechanical properties of TVGs made from PLA-PCL 70:30 treated with air plasma and coated with collagen, and they found out values of tensile modulus seven times higher than those determined in the present work for TVG3 made from plain PLA-PCL 70:30 (He et al., 2009). The reason of the significant difference in mechanical properties can be ascribed to PLA-PCL scaffold combination with collagen and post treatment with air plasma, confirming that tensile modulus strictly depends on type of polymer and its combination. As long as electrospinning technique is concerned it demonstrated to be suitable to obtain tubular vascular graft with a diameter of < 6 mm whose thickness was between 140 ± 7 μm and 175 ± 4 μm depending on the electrospinning time. SEM morphological analysis showed samples made up of fibers with suitable micrometric diameters and pore size between 5 and 35 μm.

Taking into consideration these results, PLGA and the innovative combination of PLGA blended with PHEMA and combined with PLA-PCL in a bilayered structure seemed to be the best approaches for further investigation on electrospun TVGs.

6. Conclusions

In conclusion, it was possible to successfully realize tubular vascular implants by electrospinning combining synthetic polymers with different physical–chemical characteristics. Two different approaches have been used for the realization of mono and bilayer TVGs; the bilayer TVG will be further investigated and optimized since some initial promising findings have been achieved in this research project. Future perspective is to explore different approaches in order to reduce the uncontrolled fusion of fibers during electrospinning layering process: i) high temperature of spinning room for promoting a faster solvent evaporation, ii) low flow rate of the 2nd layer in order to achieve a more slow deposition of fiber. Iii) Binary solvent mixtures having low evaporation temperature in order to achieve complete solvent evaporation and its removal from the fibers.

Declaration of Competing Interest

The authors declare that they have no known competing financial interests or personal relationships that could have appeared to influence the work reported in this paper.

References

Almasri, J., Adusumalli, J., Asi, N., Lakis, S., Alsawas, M., Prokop, L.J., Bradbury, A., Kolh, P., Conte, M.S., Murad, M.H., 2018. A systematic review and meta-analysis of revascularization outcomes of infrainguinal chronic limb-threatening ischemia. J. Vasc. Surg. 68, 624–633. https://doi.org/10.1016/j.jvs.2018.01.066.

Buscemi, S., Palumbo, V.D., Maffongelli, A., Fazzotta, S., Palumbo, F.S., Licciardi, M., Fiorica, C., Puleio, R., Cassata, G., Fiorello, L., Buscemi, G., Lo Monte, A.I., 2017. Electrospun PHEA-PLA/PCL scaffold for vascular regeneration: a preliminary in vivo evaluation. Transplant Proc 49, 716–721. https://doi.org/10.1016/j.transproceed.2017.02.017.

Catto, V., Farè, S., Cattaneo, I., Figliuzzi, M., Alessandrino, A., Freddi, G., Remuzzi, A., Tanzi, M.C., 2015. Small diameter electrospun silk fibroin vascular grafts: mechanical properties, in vitro biodegradability, and in vivo biocompatibility. Mater. Sci. Eng., C 54, 101–111. https://doi.org/10.1016/j.msec.2015.05.003.

Chen, D., Zhang, L., Zhang, W., Tang, Z., Fu, W., Hu, R., Feng, B., Hong, H., Zhang, H., 2020. Shapeable large-pore electrospun polycaprolactam cotton facilitates the rapid formation of a functional tissue engineered vascular graft. Mater. Des. 191, 108631 https://doi.org/10.1016/j.matdes.2020.108631.

Chue, W.-L., Campbell, G.R., Caplice, N., Muhammed, A., Berry, C.L., Thomas, A.C., Bennett, M.B., Campbell, J.H., 2004. Dog peritoneal and pleural cavities as bioreactors to grow autologous vascular grafts. J. Vasc. Surg. 39, 859–867. https://doi.org/10.1016/j.jvs.2003.03.003.

Cordelle, J., Mantero, S., 2020. Insight on the endothelialization of small silk-based tissue-engineered vascular grafts. Int. J. Artificial Organs 0391398820906547. https://doi.org/10.1177/0391398820906547.

Dorati, R., Chiesa, E., Pisani, S., Genta, I., Modena, T., Bruni, G., Brambilla, C.R.M., Benazzo, M., Conti, B., 2020. The effect of process parameters on alignment of tubular electrospun nanofibers for tissue regeneration purposes. J. Drug Delivery Sci. Technol. 58, 101781 https://doi.org/10.1016/j.jddst.2020.101781.

Dorati, R., Pisani, S., Maffeis, G., Conti, B., Modena, T., Chiesa, E., Bruni, G., Musazzi, U. M., Genta, I., 2018. Study on hydrophilicity and degradability of chitosan/polylactide-co-polycaprolactone nanofibre blend electrospun membrane. Carbohydr. Polym. 199, 150–160. https://doi.org/10.1016/j.carbpol.2018.06.050.

Drews, J.D., Pepper, V.K., Best, C.A., Szafron, J.M., Cheatham, J.P., Yates, A.R., Hor, K. N., Zbinden, J.C., Chang, Y.-C., Mirhaidari, G.J.M., Ramachandra, A.B., Miyamoto, S., Blum, K.M., Onwuka, E.A., Zakko, J., Kelly, J., Cheatham, S.L., King, N., Reinhardt, J.W., Sugiura, T., Miyachi, H., Matsuzaki, Y., Breuer, J., Heuer, E.D., West, T.A., Shoji, T., Berman, D., Boe, B.A., Asnes, J., Galantowicz, M., Matsumura, G., Hibino, N., Marsden, A.L., Pober, J.S., Humphrey, J.D., Shinoka, T., Breuer, C.K., 2020. Spontaneous reversal of stenosis in tissue-engineered vascular grafts. Sci. Transl. Med. 12, eaax6919. https://doi.org/10.1126/scitranslmed.aax6919.

Fioretta, E.S., Fledderus, J.O., Burakowska-Meise, E.A., Baaijens, F.P.T., Verhaar, M.C., Bouten, C.V.C., 2012. Polymer-based scaffold designs for in situ vascular tissue engineering: controlling recruitment and differentiation behavior of endothelial colony forming cells. Macromol. Biosci. 12, 577–590. https://doi.org/10.1002/mabi.201100315.

Fitzsimmons, R.E.B., Aquilino, M.S., Quigley, J., Chebotarev, O., Tarlan, F., Simmons, C. A., 2018. Generating vascular channels within hydrogel constructs using an economical open-source 3D bioprinter and thermoreversible gels. Bioprinting (Amsterdam, Netherlands) 9, 7–18. https://doi.org/10.1016/j.bprint.2018.02.001.

Fukunishi, T., Best, C.A., Sugiura, T., Shoji, T., Yi, T., Udelsman, B., Ohst, D., Ong, C.S., Zhang, H., Shinoka, T., Breuer, C.K., Johnson, J., Hibino, N., 2016. Tissue-engineered small diameter arterial vascular grafts from cell-free nanofiber PCL/chitosan scaffolds in a sheep model. e0158555-e0158555 PloS one 11. https://doi.org/10.1371/journal.pone.0158555.

He, W., Ma, Z., Teo, W.E., Dong, Y.X., Robless, P.A., Lim, T.C., Ramakrishna, S., 2009. Tubular nanofiber scaffolds for tissue engineered small-diameter vascular grafts. J. Biomed. Mater. Res. Part A 90, 205–216. https://doi.org/10.1002/jbm.a.32081.

Hu, Q., Su, C., Zeng, Z., Zhang, H., Feng, R., Feng, J., Li, S., 2020. Fabrication of multilayer tubular scaffolds with aligned nanofibers to guide the growth of endothelial cells. J. Biomater. Appl. 35, 553–566. https://doi.org/10.1177/0885328220935090.

Joy, J., Aid-Launais, R., Pereira, J., Pavon-Djavid, G., Ray, A.R., Letourneur, D., Meddahi-Pellé, A., Gupta, B., 2020. Gelatin-polytrimethylene carbonate blend based electrospun tubular construct as a potential vascular biomaterial. Mater. Sci. Eng., C 106, 110178. https://doi.org/10.1016/j.msec.2019.110178.

Konig, G., McAllister, T.N., Dusserre, N., Garrido, S.A., Iyican, C., Marini, A., Fiorillo, A., Avila, H., Wystrychowski, W., Zagalski, K., Maruszewski, M., Jones, A.L., Cierpka, L., de la Fuente, L.M., L'Heureux, N., 2009. Mechanical properties of completely autologous human tissue engineered blood vessels compared to human saphenous vein and mammary artery. Biomaterials 30, 1542–1550. https://doi.org/10.1016/j.biomaterials.2008.11.011.

L'Heureux, N., Dusserre, N., Konig, G., Victor, B., Keire, P., Wight, T.N., Chronos, N.A.F., Kyles, A.E., Gregory, C.R., Hoyt, G., Robbins, R.C., McAllister, T.N., 2006. Human tissue-engineered blood vessels for adult arterial revascularization. Nat. Med. 12, 361–365. https://doi.org/10.1038/nm1364.

Lee, S.J., Liu, J., Oh, S.H., Soker, S., Atala, A., Yoo, J.J., 2008. Development of a composite vascular scaffolding system that withstands physiological vascular conditions. Biomaterials 29, 2891–2898. https://doi.org/10.1016/j.biomaterials.2008.03.032.

Li, X., Xu, J., Nicolescu, C.T., Marinelli, J.T., Tien, J., 2017. Generation, endothelialization, and microsurgical suture anastomosis of strong 1-mm-diameter collagen tubes. Tissue Eng Part A 23, 335–344. https://doi.org/10.1089/ten.tea.2016.0339.

Li, Z., Li, X., Xu, T., Zhang, L., 2019. Acellular small-diameter tissue-engineered vascular grafts. Appl. Sci. 9, 2864. https://doi.org/10.3390/app9142864.

Matsuzaki, Y., John, K., Shoji, T., Shinoka, T., 2019. The evolution of tissue engineered vascular graft technologies: from preclinical trials to advancing patient care. Appl Sci (Basel) 9. https://doi.org/10.3390/app9071274.

McKenna, K.A., Hinds, M.T., Sarao, R.C., Wu, P.C., Maslen, C.L., Glanville, R.W., Babcock, D., Gregory, K.W., 2012. Mechanical property characterization of electrospun recombinant human tropoelastin for vascular graft biomaterials. Acta Biomater 8, 225–233. https://doi.org/10.1016/j.actbio.2011.08.001.

Nieponice, A., Soletti, L., Guan, J., Deasy, B.M., Huard, J., Wagner, W.R., Vorp, D.A., 2008. Development of a tissue-engineered vascular graft combining a biodegradable scaffold, muscle-derived stem cells and a rotational vacuum seeding technique. Biomaterials 29, 825–833. https://doi.org/10.1016/j.biomaterials.2007.10.044.

Ong, C.S., Zhou, X., Huang, C.Y., Fukunishi, T., Zhang, H., Hibino, N., 2017. Tissue engineered vascular grafts: current state of the field. Expert Rev. Med. Devices 14, 383–392. https://doi.org/10.1080/17434440.2017.1324293.

Pan, Y., Zhou, X., Wei, Y., Zhang, Q., Wang, T., Zhu, M., Li, W., Huang, R., Liu, R., Chen, J., Fan, G., Wang, K., Kong, D., Zhao, Q., 2017. Small-diameter hybrid vascular grafts composed of polycaprolactone and polydioxanone fibers. Sci. Rep. 7, 3615. https://doi.org/10.1038/s41598-017-03851-1.

Pashneh-Tala, S., MacNeil, S., Claeyssens, F., 2015. The Tissue-Engineered Vascular Graft—Past, Present, and Future, Tissue Engineering Part B: Reviews 22, 68-100. 10.1089/ten.teb.2015.0100.

Pisani, S., Dorati, R., Conti, B., Modena, T., Bruni, G., Genta, I., 2018. Design of copolymer PLA-PCL electrospun matrix for biomedical applications. React. Funct. Polym. 124, 77–89. https://doi.org/10.1016/j.reactfunctpolym.2018.01.011.

Spicer, C.D., 2020. Hydrogel scaffolds for tissue engineering: the importance of polymer choice. Polym. Chem. 11, 184–219. https://doi.org/10.1039/C9PY01021A.

Vaz, C.M., van Tuijl, S., Bouten, C.V.C., Baaijens, F.P.T., 2005. Design of scaffolds for blood vessel tissue engineering using a multi-layering electrospinning technique. Acta Biomaterialia 1, 575–582. https://doi.org/10.1016/j.actbio.2005.06.006.

Wang, D., Xu, Y., Li, Q., Turng, L.-S., 2020. Artificial small-diameter blood vessels: materials, fabrication, surface modification, mechanical properties, and bioactive functionalities. J. Mater. Chem. B 8, 1801–1822. https://doi.org/10.1039/C9TB01849B.

Wang, N., Zheng, W., Cheng, S., Zhang, W., Liu, S., Jiang, X., 2017. In vitro evaluation of essential mechanical properties and cell behaviors of a novel polylactic-co-glycolic acid (PLGA)-based tubular scaffold for small-diameter vascular tissue engineering. Polymers (Basel) 9. https://doi.org/10.3390/polym9080318.

Wise, S.G., Byrom, M.J., Waterhouse, A., Bannon, P.G., Ng, M.K.C., Weiss, A.S., 2011. A multilayered synthetic human elastin/polycaprolactone hybrid vascular graft with tailored mechanical properties. Acta Biomaterialia 7, 295–303. https://doi.org/10.1016/j.actbio.2010.07.022.

Wu, J., Hu, C., Tang, Z., Yu, Q., Liu, X., Chen, H., 2018. Tissue-engineered vascular grafts: balance of the four major requirements. Colloid Interface Sci. Commun. 23, 34–44. https://doi.org/10.1016/j.colcom.2018.01.005.

Yalcin Enis, I., Gok Sadikoglu, T., 2016. Design parameters for electrospun biodegradable vascular grafts. J. Ind. Text. 47, 2205–2227. https://doi.org/10.1177/1528083716654470.

Yuan, H., Chen, C., Liu, Y., Lu, T., Wu, Z., 2020. Strategies in cell-free tissue-engineered vascular grafts. J. Biomed. Mater. Res. Part A 108, 426–445. https://doi.org/10.1002/jbm.a.36825.

Zhang, F., Xie, Y., Celik, H., Akkus, O., Bernacki, S.H., King, M.W., 2019. Engineering small-caliber vascular grafts from collagen filaments and nanofibers with comparable mechanical properties to native vessels. Biofabrication 11, 035020. https://doi.org/10.1088/1758-5090/ab15ce.